A Light-Activated Antibody Catalyst

Matthew J. Taylor, Timothy Z. Hoffman, Jari T. Yli-Kauhaluoma, Richard A. Lerner,* and Kim D. Janda*

Contribution from the The Scripps Research Institute, Department of Chemistry and The Skaggs Institute for Chemical Biology, 10550 North Torrey Pines Road, La Jolla, California, 92037

Received July 30, 1998

Abstract: A catalytic antibody for a multistep Norrish type II photochemical reaction was investigated. Absorption of light energy by α-ketoamide substrate **1b** produced a high-energy biradical intermediate, that was then directed by the antibody microenvironment to form tetrahydropyrazine **13** with a k_{cat} of 1.4×10^{-3} min^{-1} at 280 nm irradiation and an enantiomeric excess of 78%. Antibody-catalyzed reactions performed with radiolabeled substrate indicated that little self-inactivation (6.8 mol % covalent modification after four turnovers per antibody) occurred. The singular product obtained in the antibody-catalyzed reaction was not observed in the uncatalyzed reaction unless the pH was lowered below 4. Studies suggested that the interplay of conformational control and chemical catalysis were responsible for the high specificity. A change in protonation state of the antibody was correlated with the inclusion of a new reaction pathway in the antibody-catalyzed reaction, indicating that general-base catalysis was involved in the rerouting of the Norrish reaction to form **13**. An X-ray crystal structure of the substrate was obtained and suggested that the antibody binds the α-ketoamide in a twisted conformation optimal for the first step of the photochemical reaction. The antibody described here is a model for the evolution of light-activated enzymes and can serve as a foundation for the development of light-dependent antibody catalysts for a range of even more complex photochemical reactions.

Introduction

Nature has evolved elegant mechanisms to utilize the energy of light. These include the rhodopsin-activated enzymatic cascade in vision,[1] the initiation of electron-transfer events in photosynthesis,[2] and the electron-transfer induced fragmentation of thymine dimers in DNA repair.[3] A common mechanistic feature in the enzymes that utilize light energy to catalyze chemical reactions is that absorption of a photon by the substrate or cofactor initiates a multistep process involving one or more reactive intermediates. These enzymes, as well as others, have evolved to correctly process high-energy species including cations, anions, radical anions, and radicals.[3,4] In addition to their role in enzymatic processes, photochemical reactions have also been of interest among physical and synthetic organic chemists.[5] A well-studied example is the photochemical Norrish type II reaction of both ketones and α-ketoamides which proceeds through a biradical intermediate (Figure 1).[6] In the effort to develop a catalyst for a photochemical reaction of this type, the challenge lies in the ability to not only generate but also control the reactive intermediates such that a single product is formed.

Antibodies have been shown to catalyze a variety of reactions that involve highly reactive intermediates.[7] Notably, an antibody-catalyzed photochemical reaction involving sensitization by a tryptophan residue and a putative radical anion intermediate has been reported.[8] Also, several other antibodies have been shown to process substrates by way of carbocations.[9] To investigate catalysis of the photochemical Norrish type II reaction, we chose to utilize the α-ketoamide **1** as both the hapten and substrate (Scheme 1). A hapten−substrate approach is rarely engaged because, energetically, this tactic does not adhere to the usual transition-state stabilization approach. However, here this approach is reasonable because there is an external source of energy. Thus, we could investigate the interaction of light with a substrate susceptible to such a transformation within the confines of an antibody combining site where binding energy could perturb the reaction coordinate. In so doing, we intended to establish the fate of a biradical intermediate, determine reaction pathways and product distributions, and assess the effects of chemical catalysis in the antibody microenvironment. In this regard, self-inactivation of enzymes that catalyze reactions via reactive intermediates has been observed during the turnover of alternate substrates.[10] Furthermore, while sensitization of the Norrish reaction by a tryptophan residue fortuitously present at the active site would not be expected, this did not preclude the participation by other amino acids. Significantly, pH has been shown to affect the product outcome

* To whom correspondence should be addressed.

(1)) Stryer, L. *Cold Spring Harbor Symp. Quant. Biol.* **1988**, *53*, 283 and references therein.

(2) Deisenhofer, J.; Michel, H.; Huber, R. *Trends Biochem. Sci.* **1985**, *10*, 243 and references therein.

(3) Begley, T. P. *Acc. Chem. Res.* **1994**, *27*, 394 and references therein.

(4) (a) Retey, J. *Angew. Chem., Int. Ed. Engl.* **1990**, *29*, 355. (b) Walsh, C. *Enzymatic Reaction Mechanisms*; W. H. Freeman and Company: New York, 1979.

(5) Turro, N. J. *Modern Molecular Photochemistry*; Benjamin/Cummings: Menlo Park, CA, 1978.

(6) (a) Norrish, R. G. W. *Trans. Faraday Soc.* **1937**, *33*, 1521. (b) Bamford, C. H.; Norrish, R. G. W. *J. Chem. Soc.* **1935**, 1504. (c) Åkermark, B.; Sjoberg, B.; Johansson, N.-G. *Tetrahedron Lett.* **1969**, 371.

(7) (a) Schultz P. G.; Lerner, R. A. *Science* **1995**, *269*, 1835. (b) Keinan, E.; Lerner, R. A. *Isr. J. Chem.* **1996**, *36*, 113.

(8) Jacobsen, J. R.; Cochran, A. G.; Stephans, J. C.; King, D. S.; Schultz, P. G. *J. Am. Chem. Soc.* **1995**, *117*, 5453.

(9) (a) Li, T.; Janda, K. D.; Ashley, J. A.; Lerner, R. A. *Science* **1994**, *264*, 1289. (b) Li, T.; Janda, K. D.; Lerner, R. A. *Nature* **1996**, *379*, 326.

(10) (a) Hamilton, J. A.; Yamada, R.; Blakley, R. L.; Hogenkamp, H. P. C.; Looney, F. D.; Winfield, M. E. *Biochemistry* **1971**, *10*, 347. (b) Kulmacz, R. J. *Arch. Biochem. Biophys.* **1986**, *249*, 273.

10.1021/ja982711r CCC: $15.00
Published on Web 11/21/1998

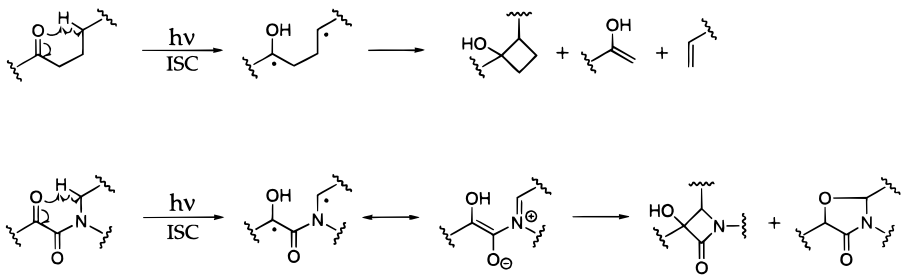

Figure 1. Mechanism of the Norrish type II reactions of ketones and α-ketoamides. Following absorption of a photon, intramolecular hydrogen atom abstraction results in the formation of a triplet biradical which undergoes intersystem crossing (ISC) to the singlet state. In the case of the α-ketoamide, the electronic configuration is in resonance with the zwitterionic and biradical state. This is usually followed by cyclization (in both cases) or fragmentation (in the case of ketones).

Scheme 1[a]

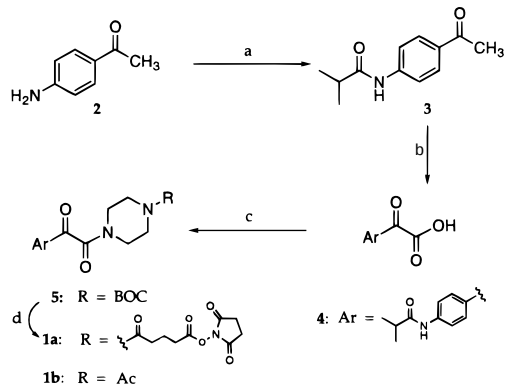

[a] (a) ^{i}BuCl, Et_3N, CH_2Cl_2, 0 °C (96%); (b) SeO_2, pyridine, 100 °C (85%); (c) *N*-acetyl-1,4-piperizine (for 1b) (40%) or *tert*-butyl 1-piperizine-carboxylate (for 5) (98%), Et_3N, BOP chloride, $CHCl_3$; (d) i) 4 M HCl, dioxane, ii) 5-[(2,5-dioxo-1-pyrrolidinyl)oxy]-5-oxopentanoyl chloride, diisopropylethylamine (DIPEA), $CHCl_3$ (92%).

of the Norrish reaction[11a] so that general acid/base catalysis might be observed. Our rationale suggested that the utilization of a singular hapten−substrate could be a viable approach in the elicitation of antibody catalysts for a multistep Norrish type II reaction.

Results and Discussion

Hapten **1a** was synthesized in five steps from 4-aminoacetophenone (Scheme 1). The aniline substructure contained in **2** was first acylated with isobutyryl chloride (^{i}BuCl). Isolation of this amide was followed by oxidation of the methyl ketone embedded in **3** with selenium dioxide (SeO_2) in pyridine to provide the α-ketoacid **4**. Coupling of **4** to *tert*-butyl 1-piperizine-carboxylate using bis(2-oxo-3-oxazolidinyl)phosphinic (BOP) chloride afforded **5** as a white solid in 98% yield. Installation of the linker for coupling to carrier proteins keyhole limpet hemocyanin (KLH) and bovine serum albumin (BSA) was achieved by deprotection of **5** with 4 M aqueous HCl and acylation of the resulting amine with the mono-*N*-hydroxysuccinimidyl (NHS) ester of glutaric acid chloride, providing **1a**. Substrate **1b**, where the C-5 linker was replaced with an acetamide functionality, was synthesized by coupling the α-ketoacid **4** to *N*-acetyl-1,4-piperazine with BOP chloride.

High-intensity, broad band UV irradiation (centered at 340 nm) of substrate **1b** under the assay conditions (50 mM *N*,*N*-bis(2-hydroxyethyl)glycine (Bicine) pH 8.5, 5% dimethyl sulfoxide (DMSO)) produced primarily one diastereomer of the β-lactam **11** and equal amounts of the oxazolidinone diastereomers **12**, consistent with the expected product distribution from literature precedence (Figure 2).[11] Purification on the milligram scale provided authentic standards of these products for comparison. A panel of 22 monoclonal antibodies (mAbs) elicited against α-ketoamide hapten **1a** were purified[12] and then screened under described conditions (vide supra). Interestingly, it was found that three of the mAbs (8C7, 2B6, and 1A3), of which mAb 8C7 was studied in detail, produced a single product that was not observed in the uncatalyzed reaction or in the absence of light energy. This product was identified as the tetrahydropyrazine **13**, resulting from a rearrangement of the biradical and/or zwitterionic intermediates **9** and **10**.[13] However, it was also found that **13** could be produced in the absence of antibody under acidic conditions (pH < 4). As an additional control, bovine serum albumin (BSA), a protein previously shown to bind small molecules and accelerate some reactions,[14] was utilized under identical conditions and had no effect on the photochemical reaction of the α-ketoamide substrate.

The above observations suggested that the photochemical reaction in the antibody combining site was under strict microenvironment control so as to produce a single, unique product. It should be emphasized that the specificity of mAb 8C7 was very high, especially when compared to that of the uncatalyzed reaction. This selectivity was illustrated by high-pressure liquid chromatography (HPLC) analysis of the reaction products (Figure 3). At pH 8.5 in the absence of antibody, no measurable amount of **13** was formed. Even at pH 1, only 50% of the product mixture was composed of tetrahydropyrazine **13**. Yet, virtually quantitative conversion of α-ketoamide **1b** to tetrahydropyrazine **13** was achieved by mAb 8C7. Fluorescence quenching experiments, in which a fixed concentration of antibody was titrated with increasing amounts of substrate, indicated up to 2 equiv were required before quenching was complete (data not shown). This result demonstrated the expected presence of two combining sites per antibody molecule.

(11) (a) Aoyama, H.; Sakamoto, M.; Kuwabara, K.; Yoshida, K.; Omote, Y. *J. Am. Chem. Soc.* **1983**, *105*, 1958. (b) Irradiation of solid **1b** produced a β-lactam diastereomer as the sole product, consistent with literature precedence (see: Aoyama, H.; Hasegawa, T.; Omote, Y. *J. Am. Chem. Soc.* **1979**, *101*, 5343). A control experiment at 20 mM substrate concentration, where precipitation was observed, revealed a product profile that was essentially a sum of the products resulting from solid-state and solution-state reactivity. We therefore concluded that **1b** was soluble under the assay conditions.

(12) Kohler, G.; Milstein, C. *Nature* **1975**, *256*, 495.

(13) Spectroscopic evidence is consistent with this structural assignment. An authentic standard of the tetrahydropyrazine **13** was synthesized by photolysis of **1b** in 5% water−acetonitrile with 1% trifluoroacetic acid and purified by preparative reversed-phase HPLC and preparative TLC. Further proof of the structure was obtained by derivatization through hydrogenation of the double bond in **13** with hydrogen over palladium on carbon. This produced a product identical to that obtained by reduction of the ketone in **1b** with sodium borohydride. Control experiments indicate that **13** was not produced from products **11** or **12** from the uncatalyzed reaction, suggesting that these are not intermediates in the uncatalyzed formation of **13**. Analogous reactivity in other α-ketoamides has not been reported.

(14) Hollfelder, F.; Kirby, A. J.; Tawfik, D. S. *Nature* **1996**, *383*, 60.

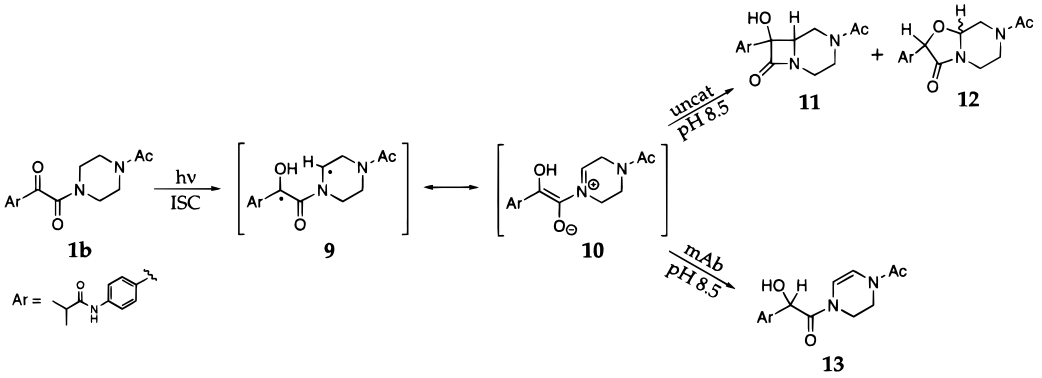

Figure 2. The products of the uncatalyzed and antibody-catalyzed reactions.

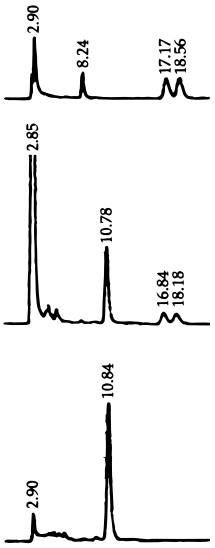

Figure 3. HPLC analysis of uncatalyzed and antibody-catalyzed reactions. The top trace is an uncatalyzed reaction at 10 μM **1b** in 50 mM Bicine, pH 8.5, 5% DMSO. Product retention times: 8.24 min (**11**), 17.17 and 18.56 min (**12**). The middle trace is from 10 μM **1b** in 0.1 N HCl, 5% DMSO. Product retention times: 10.78 min (**13**), 16.84 and 18.18 min (**12**). The bottom trace is 10 μM antibody 8C7, 10 μM **1b** in 50 mM Bicine, pH 8.5, 5% DMSO, and 9.5 μM **13** is formed.

In this initial assay, a high concentration of mAb and near stoichiometric amounts of substrate were employed to qualitatively assess product distribution. To obtain quantitative kinetic parameters, formation of tetrahydropyrazine **13** by the antibody was followed using low-intensity irradiation and catalytic amounts of antibody. Tight binding (i.e., low K_s) of substrate **1b** to the antibody prevented a full Michaelis−Menten analysis, since K_m could not be accurately determined; however, equilibrium binding constants for the substrate were obtained by BIAcore analysis[15] using **1c**. Synthesis of the amine-tethered substrate analogue **1c** was performed as shown in Scheme 2. The *N*-carboxybenzyl-γ-amino-*n*-butyric acid **6** was activated as the 1-hydroxybenzotriazole (HOBt) ester and coupled to piperazine. The resulting amine **7** was coupled to α-ketoacid **4** using BOP chloride to provide **8** in 51% yield. Following removal of the carboxybenzyl (CBZ) group, the amine was purified by preparative reversed phase HPLC to afford the trifluoroacetate (TFA) salt **1c**. A stock solution in dimethylformamide (DMF) was then utilized for immobilization of the ligand on a BIAcore chip, and BIAcore analysis was performed according to standard protocols.[15] This analysis provided a K_d = 7.6 nM. Furthermore, mAb 8C7 was shown to exhibit

Scheme 2[a]

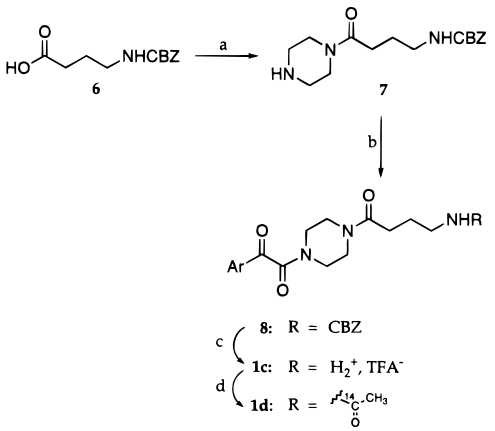

[a] (a) i) HOBt, EDC, DMF, ii) 1,4-piperizine, DMF (39%); (b) **4**, Et_3N, BOP chloride, $CHCl_3$ (51%); (c) H_2, Pd/C, EtOH (83%); (d) $CH_3{}^{14}COCl$, Et_3N, $CHCl_3$/THF (64%).

turnover and rates (measured at V_{max}) that were linear with antibody concentration. The kinetic constants were maximal at a wavelength of 280 nm,[16] giving a $V_{max} = 5.5 \times 10^{-3}$ μM/min (at 60 μM substrate, 2 μM antibody), $k_{cat} = 1.4 \times 10^{-3}$ min^{-1}, $k_{cat}/K_d = 1.8 \times 10^5$ M^{-1} min^{-1}, and a quantum yield of 0.0012. Significantly, the uncatalyzed rate of formation of **13** was not measurable under these conditions.

The effectiveness of any antibody catalyst for biradical reactions could be limited, in part, by inactivation during the course of the reaction. In studying catalytic antibodies for cationic reactions, for instance, one antibody was observed to undergo alkylation upon reaction with substrate.[17] To observe any covalent inactivation of mAb 8C7, the reaction was performed in the presence of radiolabeled substrate **1d**, synthesized by acylation of **1c** with 1-(^{14}C)-acetyl chloride. It was

(15) Malmqvist, M. *Nature* **1993**, *361*, 186.

(16) The wavelength dependence of the uncatalyzed and antibody-catalyzed reactions were examined (page S20, Supporting Information). The uncatalyzed reaction, as judged by the rate of formation of β-lactam **11**, has a wavelength versus rate maximum at 310 nm (corrected for light intensity), paralleling the absorption maximum of substrate **1b** (λ_{max} = 310 nm, ϵ_{310} = 28 000 L M^{-1} cm^{-1}). The mAb 8C7 catalyzed reaction, as judged by the rate of formation of **13**, has a rate maximum shifted approximately 20 nm to 290 nm. This shift in wavelength versus rate profile for the antibody-catalyzed reaction is most consistent with a shift in absorption maximum upon binding of substrate to antibody. The UV spectrum of the bound complex was measured; however, the spectrum is dominated by antibody absorbance in this region, making it difficult to judge whether a blue-shift in UV maximum of the substrate had occurred. An alternative model, one involving energy transfer from or sensitization by a tryptophan indole side chain (ϵ_{280} = 5000 L M^{-1} cm^{-1}) was not supported by our data, since a large contribution from substrate absorption at 310 nm in the wavelength versus rate profile would have been expected.

(17) Li, T.; Janda, K. D.; Hilton, S.; Lerner, R. A. *J. Am. Chem. Soc.* **1995**, *117*, 2367.

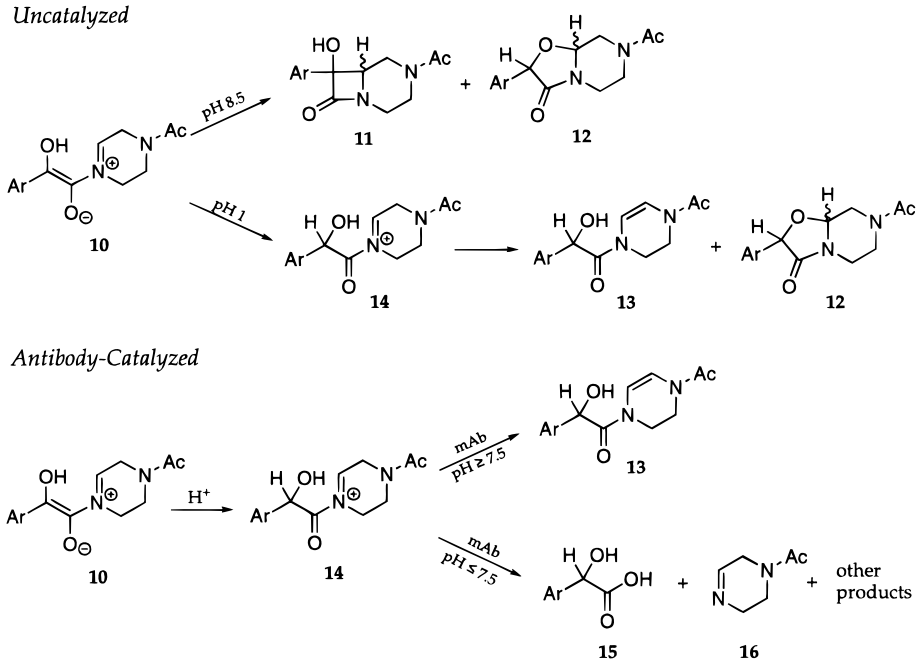

Figure 4. The pH-dependent product distributions for uncatalyzed and antibody-catalyzed reactions.

determined that after four turnovers only 6.8 mol % radioactivity remained bound per antibody molecule. This indicated that little covalent modification by the biradical intermediate occurred and that the antibody was not subject to self-inactivation during the photochemical Norrish type II reaction.

Antibody-catalyzed asymmetric induction was also examined, since a benzylic stereocenter in tetrahydropyrazine **13** was produced from the prochiral α-ketoamide **1b** during this light-driven reaction. Stereochemical control is one of the hallmarks of enzyme-catalyzed reactions,[18] and asymmetric induction has been achieved successfully in catalytic antibodies.[19] The degree of enantioselectivity was measured quantitatively by determining the enantiomeric excess (ee). To this end, the antibody-catalyzed reaction was taken to completion under stoichiometric conditions, and **13** was analyzed by chiral high-pressure liquid chromatography. Comparison to an authentic sample of racemic **13** indicated that the antibody selectively formed one enantiomer in 78% ee. The enantioselectivity was quite high, given that no stereochemistry was specified in the original hapten design. This result is perhaps most simply accommodated in terms of enantiofacial protonation of zwitterionic intermediate **10**, rather than a tantamount sequential hydrogen atom abstraction and donation by the biradical form **9**. However, the latter process cannot be ruled out. Significantly, the presence of the radical character at the prochiral carbon in this intermediate did not preclude asymmetric induction.

The pH profile for the uncatalyzed reaction revealed some important mechanistic details. In the uncatalyzed reaction at pH 8.5, there was primarily a competition between cyclization on carbon to form **11** and on oxygen to form **12**, whereas at pH 1, cyclization to **12** and proton abstraction to form tetrahydropyrazine **13** were competitive (Figure 4). This product distribution could be explained by examining the reactivity of the biradical and/or zwitterion **9** and **10**. At high pH, **10** underwent ring closure on either carbon or oxygen at a rate that apparently competed favorably with proton abstraction, since formation of **13** was not observed under these conditions. However, at low pH, protonation of **10** to form **14** competed with cyclization. Protonation can be predicted to have two effects on the reactivity of **10**. First, it is known that cyclization on carbon is disfavored under acidic conditions,[11a] which we observed as an absence of **11** at low pH. This could be attributed to a loss of both anionic and biradical character, as cyclization on carbon occurs from either **9** or **10**. Second, deprotonation of the resulting iminium ion would be favored because of an increase in the acidity of the abstracted proton, favoring the formation of **13**.

Interestingly, catalysis by mAb 8C7 exhibited a pH-dependent product distribution that strongly suggested chemical catalysis was involved in the rerouting of the Norrish reaction. A V_{max} versus pH profile for production of tetrahydropyrazine **13** was bell-shaped with a maximum at pH 7.5.[20] Importantly, the profile did not merely reflect a change in rate, but also the inclusion of a new reaction pathway. It was found that at low pH the reaction course shifted toward *fragmentation*, where it competed effectively with proton abstraction, yielding multiple products, including **15** and **16** (Figure 4).[21] A model consistent with these observations is one where a general base in the antibody combining site is performing the proton abstraction to form **13** and that, upon protonation of this basic amino acid residue, fragmentation becomes the favored process (Figure 5). It is also reasonable to presume that the antibody may use binding energy to exert conformational control over intermediates in the multistep reaction. An X-ray crystal structure for α-ketoamide **1b** was obtained and revealed a conformation where the ketone and amide carbonyls were orthogonal (Figure 6). Therefore, we assume that antibodies elicited to **1a** will bind **1b** in a twisted conformation. This geometry is optimal for the intramolecular

(18) Fersht, A. *Enzyme Structure and Mechanism*; W. H. Freeman and Company: New York, 1977.

(19) (a) Fujii, I.; Lerner, R. A.; Janda, K. D. *J. Am. Chem. Soc.* **1991**, *113*, 8528. (b) Nakayama, G. R.; Schultz, P. G. *J. Am. Chem. Soc.* **1992**, *114*, 780. (c) Zhong, G.; Hoffmann, T.; Lerner, R. A.; Danishefsky, S.; Barbas, C. F., III. *J. Am. Chem. Soc.* **1997**, *119*, 8131.

(20) Cleland, W. W. *Adv. Enzymol.* **1977**, *45*, 273.

(21) Co-injection in the HPLC assay of the products of the antibody-catalyzed reaction (50 mM MES, 100 mM NaCl, pH 6.0) with an authentic standard of **15**, synthesized by sodium borohydride reduction of the α-ketoacid **4**, suggested that fragmentation was occurring. Due to a lack of UV absorbance and/or stability, **16** was not observed in the HPLC assay, and it is important to note that two other unidentified products are also formed.

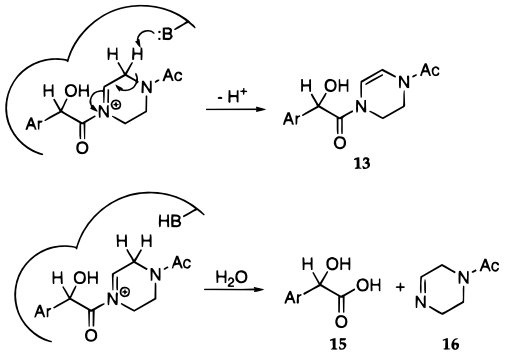

Figure 5. A model for the pH-dependent mechanism of formation of products by mAb 8C7.

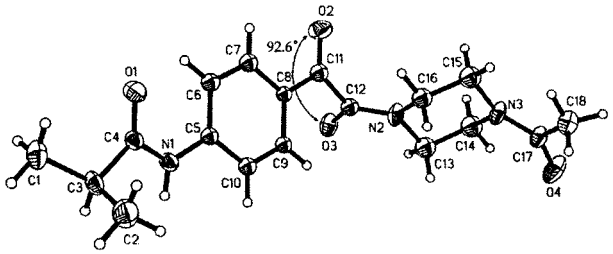

Figure 6. An ORTEP view of the X-ray crystal structure of substrate **1b**.

hydrogen atom abstraction in the photochemical reaction,[22] and rationalizes the observed successful reaction in the antibody combining site. Furthermore, calculations suggest that the ideal geometries for resonance forms **9** and **10** are nonplanar and planar, respectively.[23] Hence, the zwitterionic form should be destabilized by the antibody. It is known that **11** is preferentially formed from biradical **9** and this transformation was not catalyzed by the mAb. The observed reactivity is best explained by rapid, enantioselective protonation of an intermediate twisted structure with zwitterionic character to form the nonplanar intermediate **14**.[24] This could occur through antibody-mediated conformational destabilization of the zwitterion **10**, effectively lowering the transition-state energy for protonation to form **14**. Upon formation of **14**, deprotonation and fragmentation compete effectively with cyclization on oxygen, as formation of **12** was not observed. The behavior at high pH, where the sole product was **13** and the reaction rate decreased, was more complicated to interpret. We could speculate that either substrate and/or antibody conformation or chemical catalysis was affected by deprotonation of a general acid involved in the mechanism for formation of **6**. A hydrogen bond, possibly recruited through a "bait-and-switch"[25] in the immune response by the tertiary amide carbonyl in the hapten, could increase the acidity of the abstracted proton by binding to the negatively charged enolate oxygen of **10**. This effect would be similar to that described for the formation of **13** at low pH in the uncatalyzed reaction (vide supra). It is unlikely that such a general acid also served as a specific proton source in the reaction, since we would have expected a much higher ee value for the formation of tetrahydropyrazine **13**. With regard to conformational effects, a hydrogen bond donor might position the intermediate **10** or **14** optimally for deprotonation by the general base. Upon deprotonation of this amino acid side chain, the substrate is out of alignment for efficient proton abstraction, causing a decrease in reaction rate. Alternatively, the antibody general base might not be properly positioned because of a protein conformational change at high pH.

Conclusion

Of the three light-activated enzymes known,[26,27] perhaps the best studied is DNA photolyase.[27] In this enzyme, one cofactor functions as "antenna" (a folate) and another as electron-transfer component (a flavin) in the fragmentation of thymine photodimers in duplex DNA. The wavelength range (300−500 nm) for activity is defined by the absorbance of the cofactors in the enzyme. Even so, upon removal of the cofactors the enzyme-catalyzed reaction still proceeds, albeit poorly, with a tryptophan indole side chain now acting as the electron-transfer component.[28] Consequently, this form of DNA photolyase utilizes light energy that now corresponds to tryptophan absorbance (250−300 nm). These observations suggest that two challenges existed in the evolution of light-activated enzymes. First, nature evolved a chemical mechanism intrinsic to the enzyme protein framework. In DNA photolyase, this included binding of the thymine dimer, inclusion of a proximal indole side chain for the electron-transfer step, and processing of a radical anion intermediate. Second, the enzyme then evolved the capacity to utilize wavelengths of light energy available in the environment by installing an array of cofactors. In the antibody catalyst described here, the mechanism involved binding of the α-ketoamide and the routing of a biradical intermediate to form a single, unique product through the interplay of conformational control and combining site chemical catalysis. Hence, in essence, the antibody is representative of the early evolution of a light-activated enzyme in that the chemistry is intrinsic to the protein itself without any significant tuning of the optimal wavelength range by extrinsic cofactors. The installation of additional chemical machinery, through hapten design or protein engineering, could afford light-dependent catalytic antibodies adapted to utilize specific wavelengths of light for a wide range of photochemical reactions.

Experimental Section

All reactions were performed in an atmosphere of nitrogen with a magnetic stirrer unless otherwise noted. Analytical HPLC was performed on a Hitachi L7000 series HPLC using a Vydac 201TP54 reversed phase column. Preparative HPLC was performed on a Rainin HPLC system using a Vydac 201HS1022 reversed phase column. Methylene chloride and chloroform were distilled from calcium hydride. Tetrahydrofuran (THF) was distilled from sodium/benzophenone. Methanol was distilled from magnesium. Scintillation counting was performed on a Beckman L3801 scintillation counter using ScintiVerse

(22) The optimal geometries for the Norrish type II reactions of ketones have been determined (see: Gudmundsdottir A. D.; Lewis, T. J.; Randall, L. H.; Scheffer, J. R.; Rettig, S. J.; Trotter, J.; Wu, C.-H. *J. Am. Chem. Soc.* **1996**, *118*, 6167). Both the atomic distances and bond angles obtained from the coordinates of the α-ketoamide **1b** crystal structure compare very favorably with those optimal for intramolecular hydrogen atom abstraction in the Norrish reaction of ketones.

(23) Chesta, C. A.; Whitten, D. G. *J. Am. Chem. Soc.*, **1992**, *114*, 2188.

(24) A reviewer suggested the possibility of amino acid side chains (e.g., cysteine) in the antibody combining site participating in radical chemistry with the bound substrate. We find this intriguing because the transformation shown in Figure 2 is formally equivalent to a hydrogen atom abstraction/donation process. However, we have no evidence for this mechanism and therefore chose to discuss the simpler model, exemplified in Figure 5, for the mechanism of the antibody-catalyzed reaction involving a protonation/deprotonation mechanism. X-ray crystallographic analysis, cloning, and site-directed mutagenesis would provide data bearing on this question, but since these experiments are time-consuming and large in scope, they will be the subject of future reports.

(25) Janda, K. D.; Weinhouse, M. I.; Danon, T.; Pacelli, K. A.; Schloeder, D. M. *J. Am. Chem. Soc.* **1991**, *113*, 5427.

(26) (a) Beer, N. S.; Griffiths, T. W. *Biochem. J.* **1981**, *195*, 83. (b) Heelis, P. F.; Liu, S. *J. Am. Chem. Soc.* **1997**, *119*, 2936.

(27) Sancar, A. *Biochemistry* **1994**, *33*, 2.

(28) Kim, S.-T.; Li, Y. F.; Sancar, A. *Proc. Natl. Acad. Sci. U.S.A.* **1992**, *89*, 900.

II (Fischer) as scintillant. High-intensity photolysis was performed in a Rayonet photochemical reactor with RPR-3400 bulbs. Low-intensity photolysis was performed in a SPF-500 spectrofluorometer from SLM-Amico Instruments. Beam intensity was determined using both ferrioxalate actinometry (performed according to standard protocols[29] using a Hewlett-Packard Vectra series 4 UV−visible spectrometer) and a model 70260 radiant power energy meter from Oriel Instruments. Dialysis was performed using slide-a-lyzer cassettes purchased from Pierce. Sep-pak cartridges were purchased from Waters. 1-(^{14}C)-acetyl chloride was purchased from American Radiolabeled Chemical at a specific activity of 50 mCi/mmol.

***N*-(4-Acetylphenyl)-2-methyl-propanamide (3).** 4-aminoacetophenone (2.65 g, 19.6 mmol) and triethylamine (2.73 mL, 19.6 mmol) in 70 mL of dry CH_2Cl_2 were cooled in an ice bath. Isobutyryl chloride (2.9 mL, 19.6 mmol) was added dropwise via a syringe. The reaction was stirred for 1 h at room temperature and was judged complete by thin-layer chromatography (TLC) (CH_2Cl_2). Then 100 mL of CH_2Cl_2 was added and the organic layer washed with 50 mL of 1 N HCl, 50 mL of saturated $NaHCO_3$, and 50 mL of brine. The organic layer was then dried over anhydrous Na_2SO_4 and filtered, and the solvent was removed in vacuo to provide 3.9 g **3** as a pale yellow solid (96%): ^{1}H NMR ($CDCl_3$, 500 MHz) δ 1.27 (d, 6H, J = 6.6 Hz), 2.55 (sept, 1H, J = 7 Hz), 2.57 (s, 3H), 7.47 (bs, 1H), 7.65 (d, 2H, J = 8.8 Hz), 7.93 (d, 2H, 8.5 Hz); ^{13}C NMR ($CDCl_3$, 125 MHz) δ 19.4, 26.4, 36.5, 119.0, 129.6, 132.4, 142.8, 176.1, 197.3; HRMS for $C_{12}H_{15}NO_2$ (M^+) calcd 205.1103, found 205.1180.

4-[(2-Methyl-1-oxopropyl)amino]-α-oxo-benzeneacetic Acid (4). Compound **3** (2.52 g, 12.3 mmol) and selenium dioxide (2.04 g, 18.4 mmol) in 50 mL of pyridine were heated to 100 °C for 14 h. The selenium was filtered and the orange solution concentrated in vacuo to approximately 5 mL in volume. The residue was dissolved in 100 mL of 5% NaOH and extracted with two 30-mL portions of diethyl ether. The aqueous layer was acidified with concentrated HCl and extracted with three 50-mL portions of ethyl acetate. The combined organic layers were washed with 30 mL of brine, dried over anhydrous Na_2SO_4 and filtered, and the solvent was removed in vacuo. Flash chromatography (ethyl acetate (EtOAc)/hexane/acetic acid (HOAc) 15/1/1) provided 2.46 g (85%) of **4** as a yellow solid: ^{1}H NMR (d_6-DMSO, 500 MHz) δ 1.10 (dd, 6H, J_1 = 7 Hz, J_2 = 3.3 Hz), 2.64 (dsept, 1H, J_1 = 7 Hz, J_2 = 3.3 Hz), 7.82 (dd, 2H, J_1 = 8.8 Hz, J_2 = 3.3 Hz), 7.88 (dd, 2H, J_1 = 8.8 Hz, J_2 = 3.3 Hz), 10.34 (s, 1H); ^{13}C NMR (d_6-DMSO, 125 MHz) δ 18.9, 34.7, 39.0, 118.3, 125.8, 130.5, 145.1, 166.0, 175.7, 186.9; HRMS for $C_{12}H_{13}NO_4$ (M^+) calcd 235.0845, found 235.0919.

***N*-[4-[(4-Acetyl-1-piperazinyl)oxoacetyl]phenyl]-2-methyl-propanamide (1b).** Compound **4** (888 mg, 3.78 mmol), *N*-acetylpiperazine (480 mg, 3.74 mmol), and triethylamine (0.5 mL, 3.59 mmol) were dissolved in 9 mL of dry $CHCl_3$ and cooled on ice. Bis(2-oxo-3-oxazolidinyl)phosphinic chloride (BOP chloride) (960 mg, 3.77 mmol) was added as a solid in portions. The reaction mixture was stirred for 1 h on ice, then warmed to room temperature, and stirred overnight. Then 150 mL of EtOAc was added and the organic solution extracted with 40 mL of 1 N HCl, 40 mL of saturated $NaHCO_3$, and 40 mL of brine. The organic layer was dried over anhydrous Na_2SO_4 and filtered, and the solvent was removed in vacuo. Flash chromatography (EtOAc) provided 522 mg (40%) of **1b** as a white solid: ^{1}H NMR ($CDCl_3$, 600 MHz) δ 1.27 (d, 6H, J = 7 Hz), 2.10 and 2.16 (s, 3H), 2.55 (sept, 1H, J = 7 Hz), 3.33−3.35 (m, 1H), 3.38−3.40 (m, 1H), 3.46−3.48 (m, 1H), 3.58−3.63 (m, 2H), 3.75 (s, 2H), 3.78−3.80 (m, 1H), 7.41 (bs, 1H), 7.70 (dd, 2H, J_1 = 8.8 Hz, J_2 = 2.2 Hz), 7.93 (dd, 2H, J_1 = 8.8 Hz, J_2 = 3 Hz); ^{13}C NMR ($CDCl_3$, 125 MHz) δ 19.3, 21.3, 36.9, 40.9, 41.1, 41.2, 41.4, 45.6, 45.8, 45.9, 46.2, 119.1, 119.2, 128.0, 131.1, 144.4, 165.6, 165.8, 169.1, 175.8, 189.5; HRMS for $C_{18}H_{23}N_3O_4$ (M^+) calcd 345.1688, found 345.1773.

4-[[4-[(2-Methyl-1-oxopropyl)amino]phenyl]oxoacetyl]-1-piperazineacetic acid, 1,1-Dimethylethyl Ester (5). A mixture of **4** (0.41 g, 1.74 mmol), *tert*-butyl 1-piperizine-carboxylate (0.32 g, 1.74 mmol) and *N*,*N*-diisopropylethylamine (0.61 mL, 3.49 mmol) in anhydrous $CHCl_3$ (10 mL) was cooled to 0 °C. Bis (2-oxo-3-oxazolidinyl)-phosphinic chloride (BOP chloride) (0.44 g, 1.74 mmol) was added to the stirred solution and the reaction mixture brought to room temperature and stirred for 2 h. The mixture was diluted with EtOAc (150 mL), and the organic layer was washed successively with solutions of 0.1 M HCl (50 mL), saturated $NaHCO_3$ (30 mL), and brine (2 × 50 mL). The organic layer was dried with anhydrous $MgSO_4$ and filtered, and the solvent was removed in vacuo. The residue was crystallized twice from EtOAc/hexanes to give 0.64 g (91%) of **5** as a white solid: ^{1}H NMR δ (d_6-DMSO, 300 MHz) δ 1.09 (d, 6H, J = 9.4 Hz), 1.40 (s, 9H), 2.63 (sept, 1H, J = 9.4 Hz), 3.21 (m, 2H), 3.28 (m, 2H), 3.46 (m, 2H), 3.59 (m, 2H), 7.88 (m, 4H), 10.35 (br s, 1H); ^{13}C NMR ($CDCl_3$, 150 MHz) δ 19.3, 28.2, 36.3, 41.1, 45.7, 80.6, 119.3, 127.7, 130.8, 144.8, 154.3, 165.9, 176.3, 189.8; HRMS for $C_{21}H_{29}N_3O_5$ (M^+) calcd 403.2107, found 403.2117.

***N*-[4-[[4-[5-[(2,5-Dioxo-1-pyrrolidinyl)oxy]-1,5-dioxopentyl]-1-piperazinyl]oxoacetyl]phenyl]-2-methyl-propanamide (1a).** A mixture of *tert*-Boc piperazinyl amide **5** (0.64 g, 1.59 mmol) and 4 M hydrogen chloride in 1,4-dioxane (8.0 mL, 32 mmol) was stirred at room temperature for 30 min. 1,4-Dioxane was removed in vacuo, and the crystalline residue was lyophilized to give the amine hydrochloride (0.53 g, 98%). The crude product was used without further purification (LRMS for $C_{16}H_{21}N_3O_3$ calcd 303 (M^+), found 303). A mixture of the amine hydrochloride (0.53 g, 1.56 mmol), 5-[(2,5-dioxo-1-pyrrolidinyl)-oxy]-5-oxopentanoyl chloride (0.42 g, 1.72 mmol) and *N*,*N*-diisopropylethylamine (0.57 mL, 3.28 mmol) in $CHCl_3$ (10 mL) was stirred at room temperature for 13 h. The reaction mixture was diluted with CH_2Cl_2 (100 mL) and washed with solutions of 0.5 M HCl (20 mL), saturated $NaHCO_3$ (30 mL), and brine (2 × 30 mL). The organic layer was dried with anhydrous $MgSO_4$ and filtered, and the solvent was removed in vacuo to give crude **1a** as an off-white solid. Recrystallization (EtOAc/hexanes) gave 0.76 g (92%) of **1a** as white crystals: ^{1}H NMR (d_6-DMSO, 300 MHz) δ 1.11 (d, 6H, J = 9.4 Hz), 1.72−1.90 (m, 4H), 1.95 (t, 2H, J = 8.4 Hz), 2.64 (m, 1H), 2.82 (bs, 4H), 3.22 (m, 2H), 3.28 (m, 2H), 3.41 (m, 2H), 3.61 (m, 2H), 7.79−7.92 (m, 4H), 10.38 (br s, 1H); ^{13}C NMR ($CDCl_3$, 150 MHz) δ 19.5, 20.2, 25.6, 29.7, 30.2, 30.9, 36.9, 41.3, 41.4, 41.7, 45.0, 45.5, 45.7, 45.9, 119.2, 128.3, 131.3, 144.2, 165.6, 165.8, 168.4, 169.1, 170.4, 175.6, 189.6; HRMS for $C_{25}H_{31}N_4O_8$ (M^+) calcd 515.2141, found 515.2146.

[4-Oxo-4-(piperazinyl)butyl]carbamic Acid, Phenylmethyl Ester (7). To *N*-CBZ-γ-amino-*n*-butyric acid **6** (200 mg, 0.84 mmol) and 1-hydroxybenzotriazole (HOBt) (114 mg, 0.84 mmol) in 2 mL of DMF was added 1-[3-(dimethylamino)propyl]-3-ethylcarbodiimide hydrochloride (EDC) (165 mg, 0.86 mmol). After 30 min, the reaction was judged complete by TLC (CH_2Cl_2). The resulting activated ester was added dropwise to 1,4-piperazine (360 mg, 8.4 mmol) in 1 mL of DMF. The reaction mixture was then added to 30 mL of EtOAc and the organic solution extracted with two 30-mL portions 1 N HCl. The combined aqueous layer was adjusted to pH 10 with 1 N NaOH and saturated $NaHCO_3$. The aqueous layer was extracted with four 100-mL portions EtOAc. The organic layer was then dried over anhydrous Na_2SO_4 and filtered, and the solvent was removed in vacuo to provide a yellow oil. Flash chromatography (10−25% CH_3OH/CH_2Cl_2) provided 100 mg (39%) of **7** as a pale yellow oily solid: ^{1}H NMR (d_6-DMSO, 600 MHz) δ 1.60 (quintet, 2H, J = 7.2 Hz), 2.26 (t, 2H, J = 7.4 Hz), 2.60 (dt, 4H, J_1 = 11 Hz, J_2 = 4.8 Hz), 2.99 (dt, 2H, J_1 = 5.9 Hz, J_2 = 7 Hz), 3.33 (dt, 4H, J_2 = 4.8 Hz), 4.99 (s, 2H), 7.25−7.34 (m, 5H); ^{13}C NMR (CD_3OD, 150 MHz) δ 27.5, 31.9, 42.1, 44.2, 47.1, 47.5, 48.3, 68.2, 129.7, 129.8, 130.3, 139.4, 159.7, 174.2; HRMS for $C_{16}H_{23}N_3O_3$ (M^+) calcd 305.1739, found 305.1809.

[4-[4-[[4-[(2-Methyl-1-oxopropyl)amino]phenyl]oxoacetyl]-1-piperazinyl]-4-oxobutyl]-carbamic acid, Phenylmethyl Ester (8). Compounds **4** (63 mg, 0.2 mmol), **7** (49 mg, 0.2 mmol), and triethylamine (28 μL, 0.2 mmol) were combined in 0.5 mL of $CHCl_3$ and cooled on ice. BOP chloride (51 mg, 0.2 mmol) was added and the reaction mixture stirred first on ice for 30 min and then at room temperature for 3 h. Then 25 mL of EtOAc was added and the organic layer extracted with 4 mL of 1 N HCl, 4 mL of saturated $NaHCO_3$, and 4 mL of brine. The organic layer was then dried over anhydrous Na_2SO_4 and filtered, and the solvent was removed in vacuo. Flash chromatography (EtOAc) followed by preparative TLC (two 0.5-mm plates,

(29) Murov, S. L.; Carmichael, I.; Hug, G. L. *Handbook of Photochemistry*; Marcel Dekker: New York, 1993; pp 299−305.

EtOAc, eluted with 20% CH_3OH/CH_2Cl_2) provided 54 mg (51%) of **8** as a white foam: ^{1}H NMR ($CDCl_3$, 600 MHz) δ 1.27 (d, 6H, J = 7 Hz), 1.85−1.88 (m, 2H), 2.33−2.41 (m, 2H), 2.55 (sept, 1H, J = 7 Hz), 3.24−3.27 (m, 2H), 3.32 (bs, 2H), 3.40 (bs, 1H), 3.54 (bs, 1H), 3.60 (bs, 1H), 3.72−3.74 (m, 3H), 5.00 (bs, 1H), 5.06−5.09 (m, 2H), 7.32−7.35 (m, 5H), 7.43 (bs, 1H), 7.70 (d, 2H, J = 8.8 Hz), 7.91−7.93 (m, 2H); ^{13}C NMR ($CDCl_3$, 150 MHz) δ 19.3, 25.0, 30.2, 36.4, 40.5, 41.2, 41.5, 45.3, 45.5, 45.7, 66.5, 93.0, 119.4, 127.8, 127.9, 128.0, 128.4, 131.0, 136.5, 144.8, 156.6, 165.8, 171.0, 176.2, 189.6; HRMS for $C_{28}H_{34}N_4O_6$ (M^+) calcd 522.2478, found 522.2454.

***N*-[4-[[4-(4-Amino-1-oxobutyl)-1-piperazinyl]oxoacetyl]phenyl]-2-methyl-propanamide, Trifluoroacetate Salt (1c).** Compound **8** (50 mg, mmol) was dissolved in 2 mL of EtOH and 5 mg of 10% Pd/C added. The mixture was then stirred under 1 atm H_2 for 4 h and filtered through Celite, and the solvent was removed in vacuo. Preparative HPLC (20:80 CH_3CN/H_2O w/0.1% TFA) provided 40 mg (83%) of **1c** as a clear oil: ^{1}H NMR (CD_3OD, 600 MHz) δ 1.20 (d, 6H, J = 7 Hz), 1.90−1.95 (m, 2H), 2.54 (t, 1H, J = 7 Hz), 2.61 (t, 1H, J = 7 Hz), 2.66 (sept, 1H, J = 7 Hz), 2.94−2.99 (m, 2H), 3.37−3.39 (m, 1H), 3.41−3.43 (m, 1H), 3.52−3.54 (m, 1H), 3.59−3.61 (m, 1H), 3.66−3.68 (m, 1H), 3.74 (s, 2H), 3.78−3.80 (m, 1H), 7.81 (d, 2H, J = 8.8 Hz), 7.90−7.92 (m, 2H); ^{13}C NMR (CD_3OD, 150 MHz) δ 19.8, 23.7, 23.8, 30.9, 37.2, 40.4, 42.1, 42.3, 42.9, 45.9, 46.5, 46.7, 46.9, 120.6, 129.2, 132.1, 146.9, 167.7, 167.8, 172.7, 179.1, 191.4; HRMS for $C_{20}H_{28}N_4O_4$ (M^+) calcd 388.2111, found 388.2178.

***N*-[4-[[4-[4-(14C-Acetylamino)-1-oxobutyl]-1-piperazinyl]oxoacetyl]phenyl]-2-methyl-propanamide (1d).** Compound **1c** (8.4 mg, 16.7 μmol) was transferred to a small vial with dry methanol and the solvent removed in vacuo. A small stirbar, triethylamine (100 μL, 50.2 μmol) in 100 μL of dry $CHCl_3$, and 100 μL of dry THF were added, and the reaction mixture was cooled on ice. An ampuole of 1-(^{14}C)-acetyl chloride was cooled on ice and 1 mL of dry $CHCl_3$ containing acetyl chloride (1.6 μL, 22 μmol) added to the reservoir above the reagent chamber. The top of the chamber was then broken, and the resulting solution of radiolabeled acetyl chloride in was $CHCl_3$ drawn into a syringe and added to the reaction mixture dropwise. The transfer was completed with 1 mL of $CHCl_3$. The reaction mixture was stirred for 1 h at room temperature, followed by drying in a warm bath (37 °C) with a stream of nitrogen. The dried reaction mixture was then loaded onto a 0.5-mm preparative TLC plate with CH_2Cl_2/EtOAc/CH_3OH and eluted with 20% CH_3OH/CH_2Cl_2, and the solvent was removed in vacuo to provide 4.6 mg (64%) of **1d** as a white foam. Comparison to a nonradioactive standard by TLC confirmed the identity and purity of **1d**. The specific activity of **1d**, using the relationship 1 Ci = 2.22 × 10^{12} cpm, was determined by scintillation counting to be 12.7 mCi/mmol. Spectral data for nonradioactive **1d**: ^{1}H NMR (CD_3OD, 600 MHz) δ 1.20 (d, 6H, J = 7 Hz), 1.75−1.80 (m, 2H), 1.90 and 1.93 (s, 3H), 2.40 (t, 1H, J = 7.4 Hz), 2.47 (t, 1H, J = 7.4 Hz), 2.66 (sept, 1H, J = 7 Hz), 3.16−3.22 (m, 2H), 3.36−3.38 (m, 1H), 3.40−3.42 (m, 1H), 3.52−3.54 (m, 1H), 3.57−3.59 (m, 1H), 3.67−3.69 (m, 1H), 3.73 (bs, 2H), 3.78−3.80 (m, 1H), 7.81 (d, 2H, J = 8.8 Hz), 7.92 (dd, 2H, J_1 = 8.8 Hz, J_2 = 1.8 Hz); ^{13}C NMR (CD_3OD, 150 MHz) δ 20.3, 23.0, 26.5, 31.7, 37.7, 40.4, 42.6, 42.7, 42.9, 43.3, 46.6, 47.1, 47.2, 47.5, 121.0, 129.7, 132.6, 147.3, 168.2, 168.3, 173.9, 174.0, 179.5, 191.9; HRMS for $C_{22}H_{30}N_4O_5$ (M^+) calcd 430.2216, found 430.2127.

***N*-[4-(7-Acetylhexahydro-3-oxo-5*H*-oxazolo[3,2-*a*]pyrazin-2-yl)-phenyl]-2-methyl-propanamide (12) and *N*-[4-(4-Acetyl-7-hydroxy-8-oxo-1,4-diazabicyclo[4.2.0]oct-7-yl)phenyl]-2-methyl-propanamide (11).** Compound **1b** (20 mg, 58 μmol) was dissolved in 1 mL of 1:1 CH_3CN/H_2O in a glass vial. The solution was photolyzed at 340 nm for 1 h, then approximately 10 mL of CH_3CN was added, and the solvent was removed in vacuo. The oxazolidinones **12** (7 mg) were isolated as a mixture by preparative TLC (1-mm plate, developed three times with 10% CH_3OH/CH_2Cl_2) as well as crude **11** (ca. 3 mg). The oxazolidinones were then separated by preparative TLC (0.25-mm plate, developed four times with 10% CH_3OH/CH_2Cl_2) to provide 1 mg each (5%) of the diastereomers. For high R_f diastereomer **12**: ^{1}H NMR ($CDCl_3$, 600 MHz) δ 1.24 (d, 6H, J = 6.6 Hz), 2.16 and 2.17 (s, 3H), 2.45−2.51 (m, 1.5H), 2.57 (t, 0.5H, J = 12.7 Hz), 2.99−3.02 (m, 1.5H), 3.12 (t, 0.5H, J = 11.8 Hz), 3.82 (d, 0.5H, J = 12.7 Hz), 4.11−4.17 (m, 1.5H), 4.71 (d, 0.5H, J = 10.5 Hz), 5.06 (d, 0.5H, J = 11 Hz), 5.18 (d, 0.5H, J = 8.3 Hz), 5.24 (d, 0.5H, J = 9.2 Hz), 5.30 (s, 1H), 7.22−7.24 (m, 1H), 7.36 (d, 2H, J = 8.3 Hz), 7.35−7.56 (m, 2H); ^{13}C NMR ($CDCl_3$, heteronuclear multidimensional quantum correlation (HMQC) at 150 MHz) δ 19.2, 21.5, 36.7, 39.6, 40.7, 45.3, 46.5, 52.4, 79.2, 84.2, 84.4, 119.2, 126.8; HRMS for $C_{18}H_{23}N_3O_4$ (M^+) calcd 345.1688, found 345.1732. For low R_f diastereomer **12**: ^{1}H NMR ($CDCl_3$, 600 MHz) δ 1.25 (d, 6H, J = 6.6 Hz), 2.17 and 2.18 (s, 3H), 2.47−2.57 (m, 2H), 2.98−3.03 (m, 2H), 3.86 (d, 0.5H, J = 11.8 Hz), 4.08 (dd, 0.5H, J_1 = 13.2, J_2 = 3.5 Hz), 4.11 (dd, 0.5H, J_1 = 13.2 Hz, J_2 = 3.5 Hz), 4.22 (d, 0.5H, J = 13.2 Hz), 4.74 (d, 0.5H, J = 10.1 Hz), 5.06 (dd, 0.5H, J_1 = 10 Hz, J_2 = 2.2 Hz), 5.12−5.14 (m, 1H), 5.28 (d, 1H, J = 9.7 Hz), 7.25 (bs, 1H), 7.37−7.39 (m, 2H), 7.56 (d, 2H, J = 9.7 Hz);^{13}C NMR ($CDCl_3$, HMQC at 150 MHz) δ 19.5, 21.2, 36.5, 39.5, 40.5, 45.3, 47.8, 52.8, 79.2, 83.3, 86.6, 119.4, 127.2; HRMS for $C_{18}H_{23}N_3O_4$ (M^+) calcd 345.1688, found 345.1595. For **11**, the crude material was purified by preparative HPLC to afford 1 mg (5%). For β-lactam **11**: ^{1}H NMR (CD_3OD, 600 MHz) δ 1.19 (d, 6H, J = 6.6 Hz), 1.93−1.97 (m, 0.5H), 2.06 and 2.10 (s, 3H), 2.46−2.51 (m, 0.5H), 2.57−2.58 (m, 0.5H), 2.62 (sept, 1H, J = 7 Hz), 2.98−3.14 (m, 1.5H), 3.65−3.68 (m, 0.5H), 3.78−3.89 (m, 2H), 4.41−4.50 (m, 1H), 7.44 (dd, 2H, J_1 = 15.4 Hz, J_2 = 8.8 Hz), 7.62−7.64 (m, 2H); ^{13}C NMR (CD_3OD, HMQC at 150 MHz) δ 20.0, 21.3, 37.0, 39.4, 39.6, 45.2, 46.8, 47.0, 49.3, 49.2, 49.9, 62.0, 62.4, 121.3, 128.8; HRMS for $C_{18}H_{23}N_3O_4$ (M^+) calcd 345.1688, found 345.1586.

***N*-[4-[2-(4-Acetyl-3,4-dihydro-1(2*H*)-pyrazinyl)-1-hydroxy-2-oxo-ethyl]phenyl]-2-methyl-propanamide (13).** Compound **1b** (29 mg, 84 μmol) was dissolved in 3 mL of CH_3CN and aliquoted into six glass vials. Then 150 μL of water with 1% trifluoroacetic acid was added to each vial, and the reactions were photolyzed for 30 min. The product mixture was then dried in vacuo. Two consecutive purifications by preparative TLC (1-mm plate, developed three times with 10% CH_3OH/CH_2Cl_2, then 0.5-mm plate developed five times with 10% CH_3OH/EtOAc) provided 5.9 mg (20%) of **13**: ^{1}H NMR (d_6-DMSO, 600 MHz) δ 1.07 (d, 6H, J = 7 Hz), 2.02, 2.04, 2.06, and 2.07 (s, 3H), 2.56 (sept, 1H, J = 7 Hz), 3.36−3.82 (m, 4H), 5.40−5.49 (m, 1H), 5.75−5.82 (m, 1H), 6.14 (d, 0.3H, J = 6.6 Hz), 6.31 (d, 0.3H, J = 7 Hz), 6.38−6.41 (m, 0.4H), 6.44−6.47 (m, 0.4H), 6.57 (d, 0.1H, J = 7 Hz), 6.64 (d, 0.1H, J = 7.5 Hz), 7.24−7.28 (m, 2H), 7.55−7.59 (m, 2H), 9.80 (bs, 1H); ^{13}C NMR ($CDCl_3$, 150 MHz) δ 19.6, 20.9, 21.0, 21.3, 36.7, 38.3, 38.8, 39.7, 39.9, 42.3, 43.4, 106.6, 107.5, 107.6, 109.9, 111.0, 112.2, 120.2, 120.3, 120.3, 128.1, 134.1, 138.5, 167.0, 169.0, 169.3, 175.3; HRMS for $C_{18}H_{23}N_3O_4$ (M^+) calcd 345.1688, found 345.1760.

α-Hydroxy-4-[(2-methyl-1-oxopropyl)amino]-benzeneacetic acid (15). Compound **4** (20 mg, 85 μmol) was dissolved in 1 mL of EtOH. Sodium borohydride (16 mg, 227 μmol) was added and the solution stirred for 1 h. The product mixture was then dried in vacuo and redissolved in 0.5 mL of water. The aqueous solution was extracted with three 1-mL portions of EtOAc, the combined organic layers were dried over anhydrous Na_2SO_4 and filtered, and the solvent was removed in vacuo. The residue was dissolved in 5 mL of water and loaded onto a 35-g Sep-pak cartridge, washed with 20 mL of water, and eluted with 10 mL of CH_3CN. The solvent was removed in vacuo to provide 15 mg (75%) of **15** as a white solid: ^{1}H NMR (CD_3OD, 500 MHz) δ 1.18 (dd, 6H, J_1 = 7 Hz, J_2 = 2.2 Hz), 2.61 (dsept, 1H, J_1 = 7 Hz, J_2 = 2.2 Hz), 5.06 (s, 1H), 7.40 (d, 2H, J = 6.6 Hz), 7.55 (d, 2H, J = 6.6 Hz); ^{13}C NMR (CD_3OD, 100 MHz) δ 20.8, 37.9, 75.0, 122.0, 129.3, 137.6, 140.8, 179.5, 191.4; HRMS for $C_{12}H_{15}NO_4$ (M^+) calcd 237.0899, found 237.0892.

Antibody Assays. Antibody stock concentrations were determined by UV−vis spectroscopy using 1 OD = 1.25 mg/mL at 280 nm and 1 mg/mL = 6.7 μM. For initial screening, 100 μM substrate **1b** and 20 μM antibody were dissolved in 4-mL glass vials in 50 mM Bicine, pH 8.5 with 5% DMSO. High-intensity photolysis was performed for 5- and 20-min intervals, and an aliquot of each reaction was quenched in a one-to-one ratio with an external standard (4′-fluoroacetanilide in 15% CH_3CN/85% H_2O). Analysis by analytical HPLC was then performed.

For determination of initial rates from which kinetic parameters were derived, samples were placed in 1-mL quartz cuvettes in a SPF-500C spectrofluorimeter. Irradiation was performed at specified wavelengths with a band-pass of 2.5 nm at a beam intensity of 4.2 × 10^{-9} einsteins/

min (for 280 nm). Light intensity was attenuated with neutral density filters, and it was found that both the uncatalyzed (for formation of **11**) and the antibody-catalyzed (for formation of **13**) reaction rates were linearly dependent on light intensity between 1.1×10^{-9} and 4.2×10^{-9} einsteins/min. No drop in rate was observed upon decreasing the substrate concentration; therefore the antibody-catalyzed reaction was assumed to follow saturation kinetics, and rates were taken to be at V_{max}. The number of turnovers was found to be limited by both substrate depletion and product inhibition by **12** and **13**. The maximum number of turnovers was determined by pulsing the reaction (2.5 μM antibody) with aliquots (10 μM substrate each) of substrate stock solution and then driving the reaction to completion with high-intensity irradiation. After five pulses of substrate, 11 μM of **13** was found, indicating that the reaction proceeded to two turnovers per antibody combining site before product inhibition by **12** and **13** terminated the reaction.

Light intensity from an SPF-500 spectrofluorometer was measured by both ferrioxalate actinometry and a radiant power meter from Oriel Instruments and was determined to be 3.0×10^{-5} W at 280 nm. Using the conversion factor of 4.3×10^{5} J mol photons^{-1} at 280 nm and a V_{max} value for conversion of **1b** to **13** by mAb 8C7 of 5.5×10^{-3} μM min^{-1} in a 1-mL irradiated volume, a quantum yield of 0.0012 was obtained for the reaction. For the uncatalyzed reaction, a disappearance quantum yield of 0.00076 at 280 nm was calculated using an observed rate of disappearance of **1b** at 60 μM concentration of 3.2×10^{-3} μM min^{-1}.

The pH study versus rate study was performed using 60 μM substrate, 2 μM mAb 8C7, and 5% DMSO in 50 mM 2,2-bis-(hydroxymethyl)-2,2′,2″-nitrilotriethanol (Bis-Tris) and 4-morpholineethanesulfonic acid (MES) (100 mM NaCl) pH 6.0, 50 mM phosphate buffer saline (PBS) pH 6.8, 50 mM PBS and 4-morpholinepropanesulfonic acid (MOPS) (100 mM NaCl) pH 7.4, 50 mM Bicine and *N*-(tris(hydroxymethyl)methyl)glycine (Tricine) (100 mM NaCl) pH 8.5, 50 mM Bicine and 2-(cyclohexylamino)ethanesulfonic acid (CHES) (100 mM NaCl) pH 9.2, and 50 mM CHES (100 mM NaCl) pH 10.0.

Antibody Fluorescence Quenching. Monoclonal antibody 8C7 (50 nM) in PBS pH 7.4, 5% DMSO was titrated with substrate **1b** and antibody fluorescence (excitation at 280 nm, emission at 340 nm) followed. It was found that antibody fluorescence was quenched only up to the addition of 2 equiv (100 nM) of **1b**. A control experiment using tryptophan in place of antibody demonstrated that no quenching of tryptophan fluorescence occurred upon adding **1b**, indicating that the quenching of antibody fluorescence was not due to a filter effect.

X-ray Crystal Structure Determination for 1b. The substrate **1b** was crystallized over a period of one week by vapor diffusion from acetonitrile/water to produce crystals suitable for X-ray analysis. A crystal was mounted, and data were collected with a Rigaku AFC6R diffractometer equipped with a copper rotating anode and a highly oriented graphite monochromator. Unit cell dimensions and standard deviations were obtained by least-squares fit to 25 reflections ($50 < 2\theta < 80°$). The data were corrected for Lorentz and polarization effects. The structure was solved by direct methods using SHELXS86. All calculations were done on a Silicon Graphics Personal Iris 4D/35 and an IBM-compatible PC using programs TEXSAN (data reduction), SHELXL-93 (refinement), and SHELXTL-PC (plotting). Crystal data: formula, $C_{18}H_{23}N_3O_4$; formula weight, 345.39; crystal system, orthorhombic; space group, $P2_{111}$; color, colorless; unit cell, $a = 6.051$ Å, $b = 15.928$ Å, $c = 19.031$ Å; $Z = 4$; final R value = 0.0733; goodness of fit = 1.063.

Radiolabeling Experiment. To a 2.5 μM solution (200 μL, PBS pH 7.4) of mAb 8C7 was added 10 μM (1 μL of a 2 mM stock) of **1d**. The reaction mixture was photolyzed for 20 min, followed by the addition of another aliquot (1 μL) of **1d** and further photolysis for 20 min; this procedure was repeated 3×. Control experiments containing antibody and substrate alone, as well as antibody and substrate without photolysis, were performed in parallel. All reactions were diluted 1:1 with 6 M guanidinium−HCl and heated to 55 °C for 2 h, followed by exhaustive dialysis against 100 mM ammonium acetate, pH 5.5. The dialyzed samples were then diluted into 10 mL of scintillation fluid, and the remaining activity was measured by scintillation counting. It was determined that 0.016 nmol ^{14}C (for a specific activity of 12.7 mCi/mmol) was bound per 0.5 nmol antibody combining site.

Enantioselectivity of mAb 8C7. Enantioselectivity was determined as follows: A 0.4-mL volume reaction (PBS, pH 7.4, 5% DMSO) containing 10 μM substrate and 10 μM antibody 8C7 was irradiated until no substrate remained as judged by HPLC analysis. The aqueous solution was extracted (3 × 1 mL, EtOAc), the organic phase was dried with anhydrous sodium sulfate, and then the solvent was removed in vacuo. The aqueous phase was analyzed by HPLC to verify extraction of the product (>90%), and then **13** was analyzed (injected in 35 μL of dry chloroform) on a Chiralpak HPLC column (Daicel). Conditions: 18% 2-propanol/hexane with 0.1% trifluoroacetic acid, 40 °C; retention times for enantiomers from analysis of authentic racemic **13**, 21 min, 28 min. The ratio of the difference in peak areas over the sum of the peak areas provided the ee value. It was also verified at this time that authentic standards of **11** and **12** were racemic by chiral HPLC analysis.

Acknowledgment. This work was supported by the National Institutes of Health (GM 43858) and The Skaggs Institute for Chemical Biology, and also in part by TEKES, Technology Development Centre, Helsinki, Finland (J.T.Y-K.) We thank Shenlan Mao for BIAcore analysis, Raj K. Chadha for the X-ray crystal structure determination, Professor Peter Wirsching for a critical reading of the manuscript, as well as Professor David Millar and Professor Albert Eschenmoser for helpful discussions.

Supporting Information Available: ^{1}H, ^{13}C, and HMQC (1H−13C coupled) NMR spectra for **13**, ^{1}H and HMQC NMR spectra for **1b**, **11**, and **12**, X-ray structural information for **1b**, the pH versus V_{max} plot for formation of **13** by mAb 8C7, and plots of wavelength versus rate data for the uncatalyzed and antibody-catalyzed reactions as well as plots of absorption spectra of **1b** and **1b** bound to mAb 8C7 (19 pages, print/PDF). See any current masthead page for ordering information and Web access instructions.

JA982711R